
Volume 18, issue 1
January 2011
ISSN 1350-4177
ELSEVIER
Ultrasonics
SONOCHEMISTRY
Available online at www.sciencedirect.com
ScienceDirect
http://www.elsevier.com/locate/ultsonch

Ultrasonics Sonochemistry 18 (2011) 127–134

Contents lists available at ScienceDirect

Ultrasonics Sonochemistry

journal homepage: www.elsevier.com/locate/ultsonch

Micro-emulsion under ultrasound facilitates the fast synthesis of quantum dots of CdS at low temperature

Mohammad H. Entezari *, Narjes Ghows

Department of Chemistry, Ferdowsi University of Mashhad, 91775 Mashhad, Iran

ARTICLE INFO

Article history:
Received 24 November 2009
Received in revised form 5 April 2010
Accepted 6 April 2010
Available online 9 April 2010

Keywords:
Ultrasound
Semiconductor
Crystallization
Interface diffusion
Intensity

ABSTRACT

Semiconductor nano-particles of CdS (about 2 nm) with a hexagonal phase have been prepared at a relatively low temperature (60 °C) and short time in micro-emulsion (O/W) under ultrasound. This study presents the effects of ultrasonic irradiation on the formation of CdS nano-particles in micro-emulsion and compares the results with samples prepared without sonication. The nano-particles have been characterized by high-resolution transmission electron microscopy (HRTEM), X-ray diffraction (XRD), energy dispersed analysis of X-ray (EDAX), UV–visible spectroscopy, and surface area measurements (BET). The effect of some important factors such as sonication time, intensity of ultrasound, temperature, and oil fraction was studied on the prepared nano-particles. The particle size can be controlled by applying the ultrasonic waves on the micro-emulsion under proper conditions. It has been postulated that bubble collapse generates high temperature and many nucleation sites which lead to the uniform spherical particles with small size and fast transition phase. Further evidence was obtained by UV–visible absorption and a photoluminescence spectrum. The study of optical properties reveals that the band-gap of the CdS nano-particle decreases with increase of sonication time and reach an approximate constant value. It was also observed that nano-particles grew faster at the beginning of sonication and then reached an almost constant value. The growth of nano-particles at different intervals during sonication was followed by UV–visible spectroscopy.

1. Introduction

Semiconductor nano-crystals have been widely studied in recent years owing to their unusual physical properties and the wide range of potential applications [1–3]. One of the important properties is the optoelectronic behavior of the semiconductors which is often strongly dependent on their particle size, morphology and crystal phases. In semiconductors with very small size, quantum confinement modulates the band structure of nano-particles and increases the band-gap [4]. The control of nano-particles' properties is significant for many technological applications such as light-emitting diodes [5], photocatalysts [6], biological labels [7], electrochemical cells [8], lasers [9], and microcavities [10]. Among the II–VI semiconductors, CdS is of special interest because it exhibits high photosensitivity and its band-gap energy (2.4 eV) appears in the visible spectrum [11]. Cadmium sulfide as a semiconductor is useful in applications such as optoelectronics [12], photocatalysis [7], and photo-degradation of water pollutants [13,14]. Various techniques have been successfully developed for the synthesis of CdS nano-crystals. The important methods used are electrochemical methods [15], gamma-irradiation [16], solvo-hydrothermal [17], thermal evaporation [18,11], microwave [19], micro-emulsion [20–22] and ultrasonic method [23].

Micro-emulsion processing has been proven to be an effective way for the controlled growth of inorganic nano-particles [24,25] with narrow size distribution and good mono-dispersity. This is due to its ability to stabilize the clusters and thus inhibit their indefinite growth. In addition, it is a gentle technique and does not require special instruments or extreme conditions [26]. The products of micro-emulsion process are particles with poor crystallinity. Therefore, to improve the crystal phase of the products it is necessary to use relatively high temperatures and long reaction times (above 300–400 °C) [17]. Hence, it seems that the combination of ultrasound and micro-emulsion is very suitable for synthesis of CdS nano-particles. This combination could be useful for controlling of crystal phase, morphology, and the size of the nano-particles.

In the present work, we have used a combined method of ultrasound and micro-emulsion which is called sono-micro-emulsion method for the synthesis of CdS nano-particles. Sonochemical processing has an important role in this kind of research which is due to the fact that this approach can in principle generate novel materials with unusual properties [23] such as metals [27], metal carbides [28], metal oxides [29], and metal chalcogenides [30,31]. Acoustic cavitation produced by ultrasonic waves can strongly

---

* Corresponding author.
E-mail address: moh_entezari@yahoo.com (M.H. Entezari).

1350-4177/$ - see front matter © 2010 Elsevier B.V. All rights reserved.
doi:10.1016/j.ultsonch.2010.04.001

increase the surface area and mass transfer between two phases, both of which enhance the diffusion coefficient on the interface mixing better than conventional agitation [32,33].

There are relatively few reports on the formation of nano-particles using the combination of ultrasound and micro-emulsion [34]. The sonochemical formation of CdS nano-particles have been reported with a hexagonal structure in the range of 80–120 nm in CS_2–water–ethylenediamine micro-emulsion [35]. Wang et al. have prepared CdS nano-particles with a cubic structure by a sonochemical method in an O/W micro-emulsion [36]. De et al. have synthesized semiconductor nano-particles (CdS and ZnS) in W/O media and reported that the photo-absorption threshold of semiconductors increases as the H_2O content of reverse micelles increases [37].

2. Experimental section

2.1. Materials

Ethylenediamine, sulfur, *p*-xylen, CTAB and 1-butanol from Merck and $CdCl_2$, $2H_2O$ from Fluka have been used without further purification. De-ionized water was used for the sample preparation.

2.2. Synthesis of nano-particles

First, 1000 mg of sulfur was dissolved in 50 ml of *p*-xylen at about 313 K. Then, a quaternary oil-in-water micro-emulsion formed by CTAB/1-butanol/*p*-xylen/water with a proper ratio and used as a reaction medium for CdS nano-particles preparation. The composite of micro-emulsion was set with weight ratio between oil and CTAB, water and oil, co-surfactant and surfactant at 0.6, 44, and 2, respectively. The micro-emulsion was prepared in two separate parts (A = 80% and B = 20% w/w). The A portion contained sulfur (37.8 mg) in oil phase and the B portion contained cadmium chloride (0.025 M) and ethylenediamine (0.41 M) in the aqueous phase of the micro-emulsion. The clear micro-emulsion of B was added slowly into the clear micro-emulsion of A. The mixed micro-emulsion was stirred by stirring and Heidolph homogenizer DIAX 900 separately and it was heated to about 60 °C for 30 min without sonication. In another experiment, the above-mentioned mixture of micro-emulsion was irradiated with ultrasound (20 kHz Sonifier W-450, output acoustic power 45.5 W (amplitude 75%), horn with 1.9 cm diameter) for 30 min (Fig. 1). During sonication, the temperature was increased from 30 to 60 °C by stopping the circulating bath. Nucleation processes began immediately and after 5 min a large amount of nuclei was formed. The precipitate was separated by centrifugation, washed with distilled water and then 2–3 times with absolute ethanol for removing the excess surfactant, and then dried in dessicator at room temperature.

2.3. Characterization of CdS nano-particles

The structure and morphology of the final products has been studied by transmission electron microscopy (HRTEM), Hi-TEM is Hitachi 300 kV H-9500 TEM with accelerate voltage 300–100 kV and resolution 0.1 nm for the crystal lattice and 0.18 for point to point, X-ray diffraction (XRD) patterns were recorded in a wide angle range ($2\theta = 10–70°$) by Bruker-axs, D8 Advance in scanning step of 0.02°/s, with monochromatized Cu Kα radiation ($\lambda = 1.5406$ Å). The energy dispersed analysis of X-ray (EDAX) was carried out using a Philips, XL30 model, and the surface area measurement (BET) was done by MONOSORB and the out-gassing of the samples were carried out at 100 °C for 3 h. The optical properties of the nano-particles were studied by UV–visible spectroscopy (Unico 2800).

3. Results and discussion

In the present study, it is confirmed that ultrasonic irradiation would favor the formation of the hexagonal phase of CdS and facilitates the phase transition at relatively low temperature. The effect of important factors such as sonication time, intensity of ultrasound, oil fraction, and temperature was studied on the CdS nano-particles.

The nature and morphology of the metal sulfides depend on the preparation conditions [17,38]. In the present work, sulfur

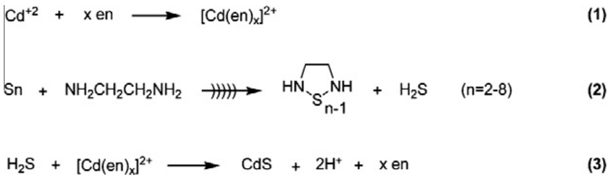

Scheme 1. Suggested reaction steps.

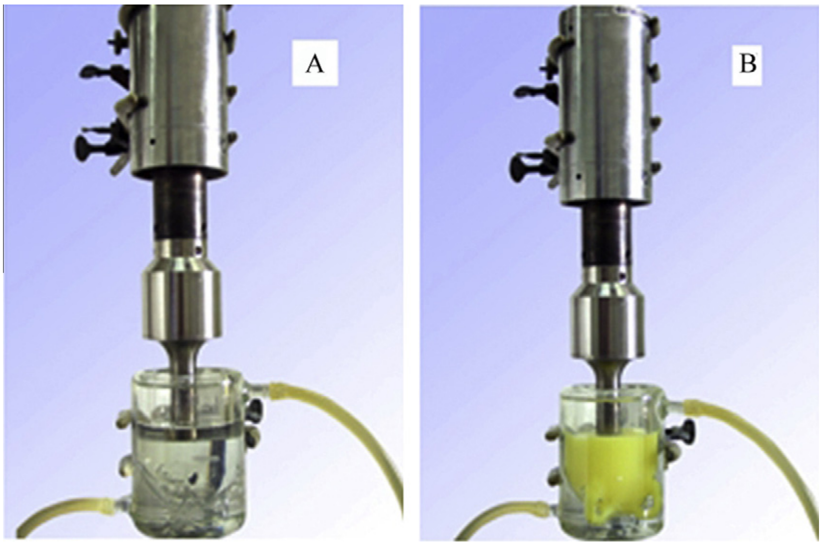

Fig. 1. Showing the experimental set up: (A) 0 min and (B) 30 min.

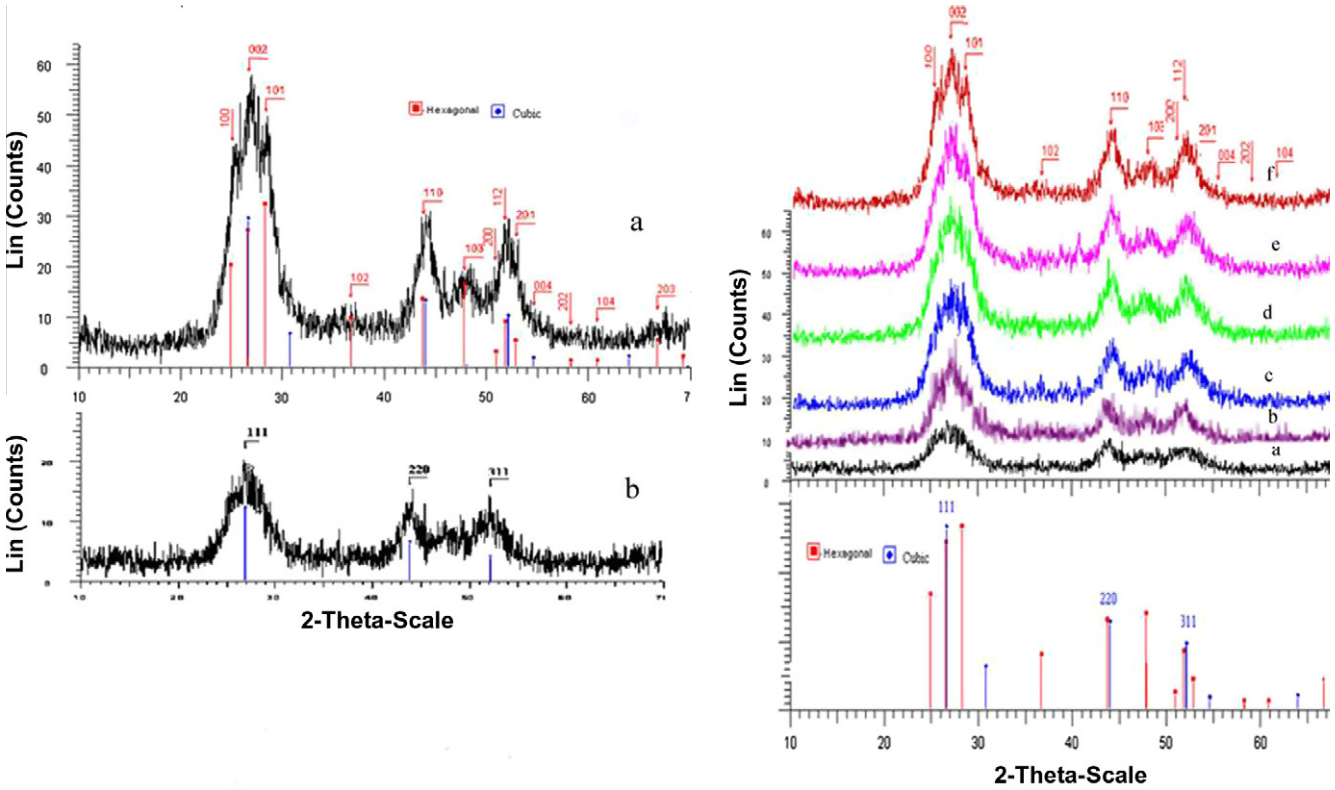

Fig. 2. X-ray diffraction patterns of the prepared CdS in: (a) sonication, 45 min; (b) stirring, 30 min. *Insert:* X-ray diffraction patterns of the prepared CdS in (a) stirring, 30 min; (b) homogenizer at 11,000 rpm, 30 min; (c) sonication, 5 min; (d) sonication, 15 min; (e) sonication, 30 min and (f) sonication, 45 min.

powder was dissolved in *p*-xylen as the oil phase, ethylenediamine (en) and cadmium chloride were dissolved in the aqueous phase. The formation of cadmium sulfide nano-particles is based on the reaction between sulfur and ethylenediamine which were present in two different phases. Ultrasound facilitates the approach of these two species by increasing the diffusion and promotes the reaction to produce H_2S. Then hydrogen sulfide quickly reacts with cadmium ion and leads to CdS (Scheme 1 [30]). In contrast to the classical method, the nucleation process in the sonication method was begun immediately and after 5 min a large number of nuclei were formed. As the size of the particles is small, it should be assumed that the nuclei were wrapped by the surfactants to prevent their aggregation. The wrapped CdS nuclei were automatically dispersed in the whole aqueous phase by the ultrasound.

Fig. 2 displays the XRD patterns of CdS nano-particles prepared in the presence and absence of ultrasound. This pattern provides information on the crystalline phase of the nano-particles, as well as on the particle size. The broad peaks indicate that the crystallites are nano-size. According to the full width at half-maximum (FWHM) of the longest diffraction peak which is due to 0 0 2 plane, the average size of nano-crystals are 2.1, 2.6 and 2.4 nm in the presence and absence of ultrasound (stirring and homogenizer), respectively. The size of the particles (Table 1) is calculated based on the Scherrer equation. The diffraction peaks for the hexagonal phase are due to (1 0 0), (0 0 2), (1 0 1), (1 1 0), (1 0 3), (1 1 2) planes (JCPDS code 41-1049), and for the cubic phase are related to (1 1 1), (2 2 0), (3 1 1) planes (JCPDS code 10-0454). The XRD patterns indicate that the nano-particles are mostly in the hexagonal phase in the presence of ultrasound and in the cubic phase in the absence of ultrasound.

According to the literature, the transition from cubic to the hexagonal phase occurred in the range of 160–240 °C by the hydrothermal method [17]. In the present work, ultrasound facilitates the phase transition at relatively low temperature. On the other hand, Fig. 2 shows that the sharpness of the XRD peaks is higher for sonication than the two other methods. Enhancing the crystal phase of the CdS in the presence of ultrasound would be explained as a result of the cavitation process. The chemical and physical effects of ultrasound arise from acoustic cavitation. When a bubble is formed in a micro-emulsion system, there is a possibility for small droplets of oil to accumulate at the interface of the bubble produced by ultrasound. This behavior arises from the higher tendency of the oil droplets to the bubble interface than water phase. The implosion of a bubble generates many local hot spots in the solution and promotes the reactions. The formation, growth and crystallization of CdS nuclei are accelerated under these conditions (Fig. 3). The high temperature produced during the cavitation can facilitate the crystallization of the product. It means that the hot spots produced during sonication play a role the same as a calcination process.

The HRTEM of nano-particles is presented in Fig. 4a and b. It shows that nano-particles have uniform spherical morphology and their sizes are very small. The crystallinity of the product has also proven by HRTEM. The results of optical and XRD measurements confirm that the sizes are under 5 nm which means the formation of quantum dots (Table 1). Table 1 shows that the size of the particles is almost similar but the surface area measured by BET (Fig. 4c) is different which might be due to the surface of the particles. This is similar to the observations made by Grinstaff et al. [39] who prepared Fe powder by sonication of $Fe(CO)_5$ [40].

It is interesting that the hexagonal phase was obtained at very low temperatures (60 °C) and short times (5 min) in our combined method (Fig. 2). Ultrasound has decreased the size of the particles relative to the particles prepared by the two other methods. This

Table 1
XRD characteristics of the prepared CdS with ultrasound at different interval times.

Sonication time (min)	Max. int. (cps)	FWHM 2θ	*h k l*	*d* (obs. max.) (Å)	Obs. max. 2θ	Size (nm)
10	45.8	3.899	0 0 2	3.2754	27.204	2.19
15	48.3	4.243	0 0 2	3.2829	27.141	2.05
30	54.3	4.046	0 0 2	3.2972	27.021	2.10
45	54.4	4.045	0 0 2	3.3031	26.972	2.11
30 (homogenizer (11,000 rpm))	36.8	3.570	1 1 1	3.3090	26.920	2.40
30 (classic)	19.0	3.297	1 1 1	3.2832	27.139	2.60

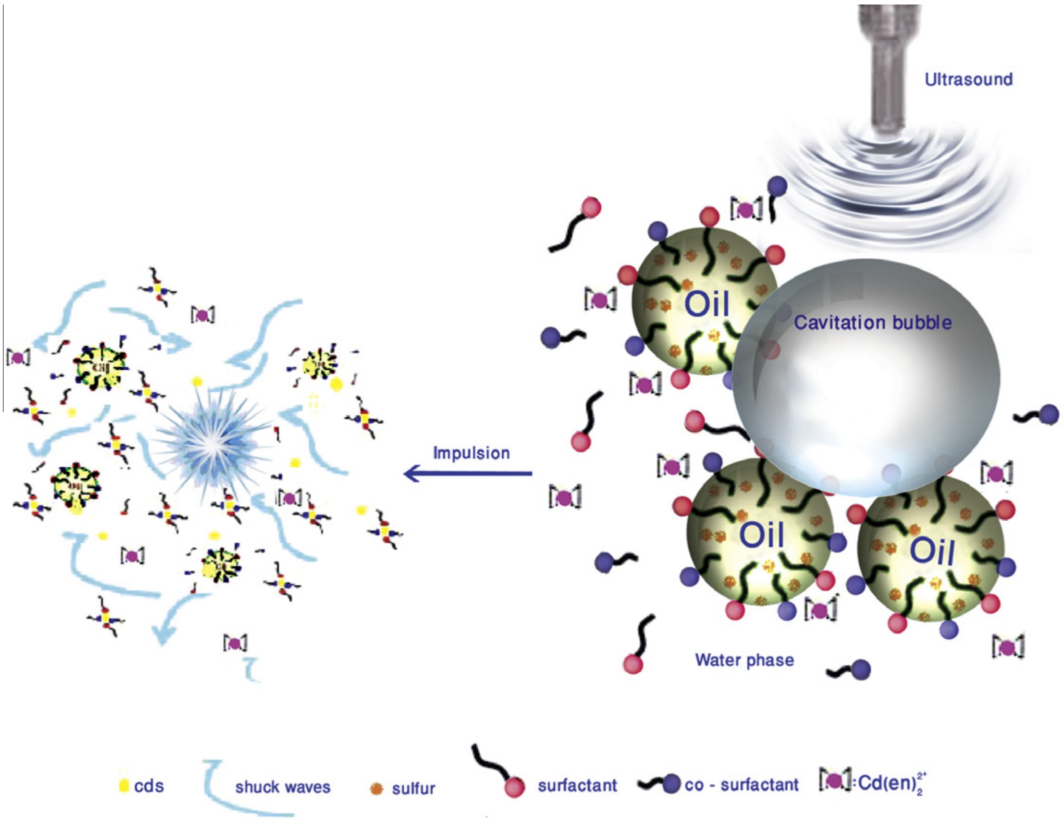

Fig. 3. Proposed reaction mechanism.

has been explained that the ultrasound irradiation increases the number of dispersed phase droplet by disrupting the droplets to smaller one. Then it increases the sites of nucleation and results to the smaller particles [34,41].

Ultrasound can also promotes the reaction of ethylenediamine in water phase with sulfur in organic phase to produce H_2S at the oil–water interface. Thus the size of the CdS nano-particles is almost related to the rate of formation of hydrogen sulfide. This fact implies that the rate of reaction strongly affects the nucleation process of the CdS nano-particles. The total number of nano-particles is correlated with the number of nuclei formed in the solution. The number of nuclei also corresponds to the rate of hydrogen sulfide formation [42]. In addition, no excessive sintering or growth of the particles is seen. This indicates that the nano-particles that are formed remain stable during the sonication process.

The results of EDAX measurement (sonication, 10 min) reveal that the CdS nano-crystals that were prepared have a high purity and the average atomic ratio of Cd:S is 50.50:43.87, which points out that the surface of the product is slightly richer in Cd. The remaining (5.63) is related to the titanium from the horn of apparatus (Fig. 5).

3.1. Intensity of ultrasound

On the basis of the results in Fig. 6, the surface area of the nano-particles is dependent on the intensity of ultrasound. As it is shown, by increasing the intensity of ultrasound the surface area of nano-particles increased and then decreased. Therefore, there is an optimum intensity for higher surface area. This behavior could be explained by the cavitation process. As the main factor for the preparation of CdS is the formation of hydrogen sulfide, the intensity of ultrasound affects the rate of production of hydrogen sulfide through the cavitation process. It is also strongly influences the nucleation process and the following formation steps of the CdS nano-particles. It is known that the acoustic intensity can influence the number of cavitation bubbles produced during the sonication. The number of cavities increases with increasing acoustic intensity until it reaches to the certain intensity which is related to the properties of the medium. Further increasing the intensity produces less effect which is due to the coalescence of the bubbles. The produced enlarged bubbles float to the surface of the liquid and can not affect more on the process. Therefore, the surface area reduced in higher acoustic intensity.

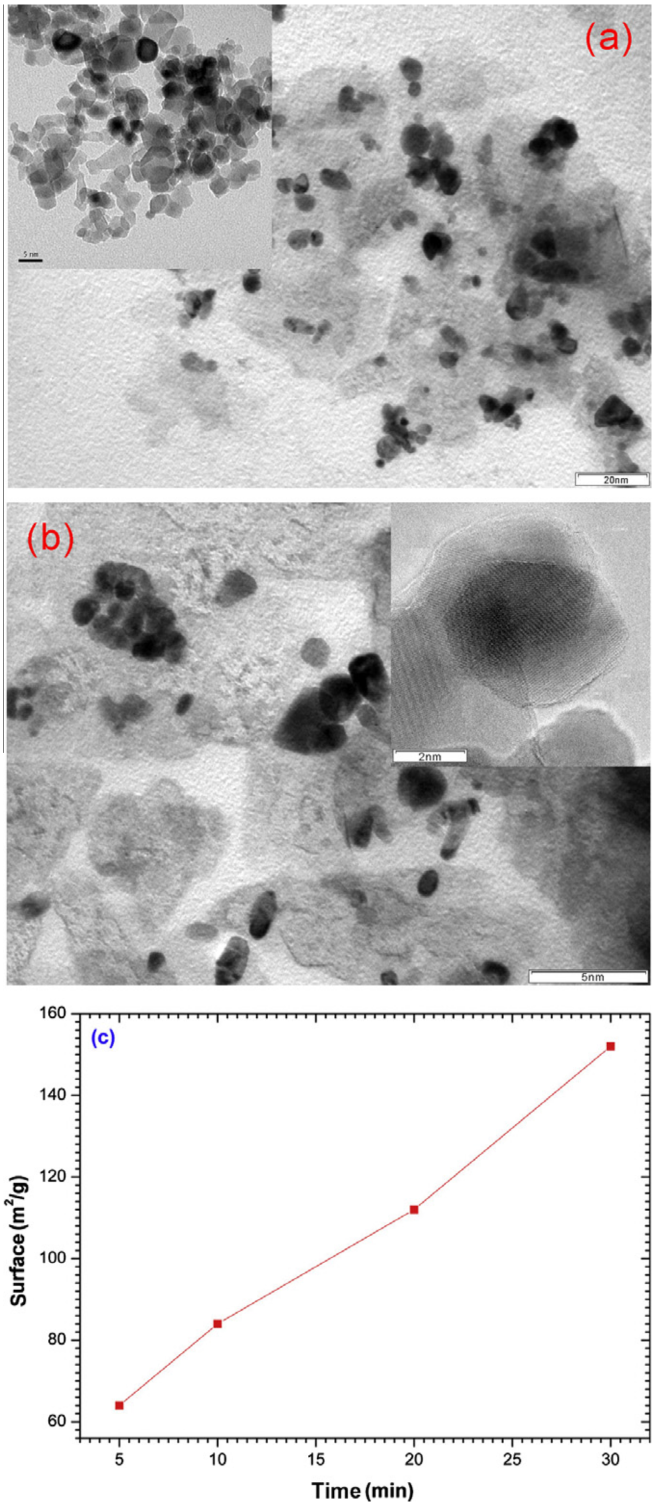

Fig. 4. HRTEM images of the prepared CdS: (a) stirring, 30 min; (b) sonication, 30 min and (c) surface area versus time.

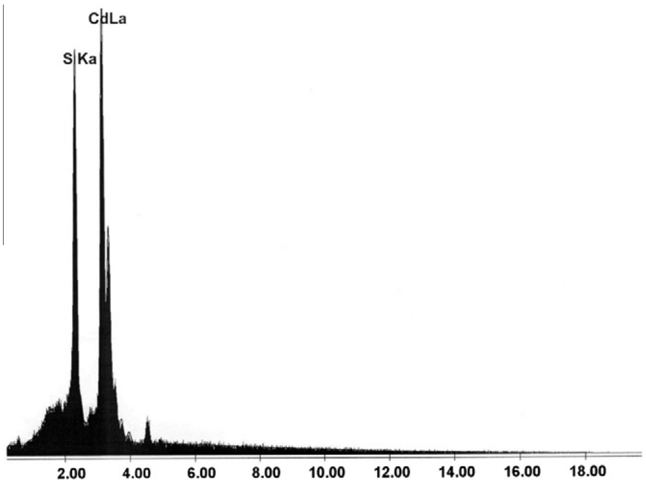

Fig. 5. EDAX measurement of the prepared CdS nano-crystals.

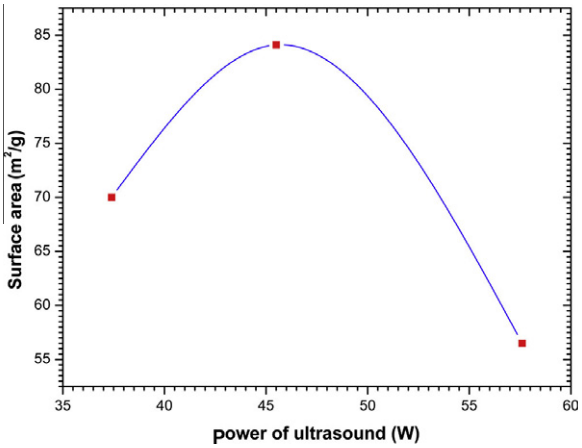

Fig. 6. Effect of intensity of ultrasound on nano-particles in 10 min of sonication.

3.2. Oil fraction

In micro-emulsion, the control of particle size and composite depends on many parameters. One of the important factors is the amount of oil fraction in the solution. This parameter was investigated with changing the oil fraction from 0.022 to 0.048 by keeping constant the amount of other constituents. The particle size increased and the surface area of the particles decreased with increasing the oil fraction in the solution (Table 2). This should be explained that with increasing the oil fraction in constant amount of sulfur, the concentration of sulfur reduced. Therefore, the rate of product formation reduced and leaded to the larger particles. In addition, the size of oil droplets in micro-emulsion can increase by increasing the oil fraction.

3.3. The effect of temperature

Another important factor is the effect of temperature on the nano-particle's growth in the micro-emulsion. The experiments were conducted by sonication of micro-emulsion at two different temperatures. The results (Table 3) show that both the final size and the surface area of the nano-particles are affected by temperature. An increase in temperature leads to a higher mass transfer between two phases and enhances the reaction rate [21].

3.4. Optical properties

UV–visible absorption spectroscopy is a useful technique to monitor the optical properties of the quantum-sized particles. The UV–visible spectra of samples at different interval times are shown in Fig. 7a. The maximum absorption for CdS as a bulk material is around 515 nm (2.4 eV) [43]. Therefore, according to Fig. 7a

Table 2
Effect of oil fraction on the surface and size of nano-particles in 10 min sonication.

Weight ratio O/W	Weight ratio O/Sur.	Size crystal (XRD) (nm)	Optical size (nm)	Band-gap (eV)	Surface (m^2/g)
0.022	0.59	2.19	4.60	2.73	84.1 ± 0.3
0.048	0.60	2.23	4.78	2.70	75.0 ± 0.7

Table 3
Effect of temperature on the surface and size of nano-particles in 30 min sonication.

Temperature (°C)	Size crystal (XRD) (nm)	Optical size (nm)	Band-gap (eV)	Surface (m^2/g)
60	2.10	4.66	2.72	152 ± 1
80	4.00	5.64	2.60	124 ± 2

the CdS nano-materials have shown an obvious blue-shift which is due to quantum confinement. In addition, the observed optical absorption edges are almost equal but show a little red-shift at longer times. The difference between the absorption onset and the absorption maximum characterizes the width of the particle size distribution [44]. Therefore, CdS nano-crystals obtained in this work have a relatively narrow size distribution.

The band-gap of different samples has estimated using the "knee" method [45,46] and the particle size calculated using effective mass approximation (EMA) [47]. Fig. 7b shows that the band-gap shifts to lower energies very fast at the beginning of sonication and then changes with time slowly. The opposite behavior is seen for the particle size. In initial times (5 min), the size of nano-particles increases to 4.33 nm while from 10 to 45 min of sonication, the size increases by only 0.15 nm. This range of sizes might be attributed to the over-estimation of the EMA approximation for the particles smaller than 6 nm that yields optical sizes larger than XRD sizes. In this regard, the XRD sizes are expected to be more realistic than the optical sizes. The uncertainty in XRD sizes is due to the non-ideal size averaging over a distribution of sizes, as well as the instrumental broadening. The uncertainty in XRD size has been reported to be less than 0.5 nm in several papers, where the size from HRTEM is considered as the true size [48]. Fig. 7c shows the photoluminescence spectrum of CdS nano-particles with a large blue-shift due to quantum size effects. There is no emission peak at about 600 nm associated with the defects and impurities in CdS nano-crystals [43]. This confirms the high crystallinity and purity of the nano-particles. A weak shoulder peak at 400 nm (this peak is perhaps due to split of continuous energy bands of the nano-particles into discrete levels [4] which lead to allow energy transfer higher than the band-gap energies) and a relative sharp emission peak appeared at about 480–490 nm that is located near the absorption band edge. The latter one can attribute to electron–hole pair recombination at surface trap states [49]. The latter emission is strong, suggesting that the synthesized CdS nano-particles are likely rich with respect to Cd^{2+} than S^{2-}, as observation in EDAX measurements, can result in higher fluorescence quantum yields [50].

The exitonic shoulder and sharp absorption edge is indicative of highly mono-disperse particles with narrow size distribution and good crystallinity in the presence of ultrasound (Fig. 8). But in the other methods the slope of the absorption band is not very steep, and this is due to the relatively low mono-dispersity of the nano-particles. The obtained results are summarized in Table 4.

4. Conclusions

In conclusion, in the present work we have developed a new method to synthesize CdS nano-particles through combination of ultrasonic waves and O/W micro-emulsion. Nano-particles with a hexagonal structure were prepared at a relatively low temperature (60 °C), short time, and fast transition phase. The advantages of this combined method are due to its simplicity and efficient way for preparation of very fine nano-particles (quantum dot) with uniform shape. During cavitation, bubble collapse produces strong shock waves and intense local heating that leads to an increase mass transfer and diffusion of species to each other and enhances the crystallinity of the produced nano-particles. The surface area of nano-particles was increased with increasing the sonication time.

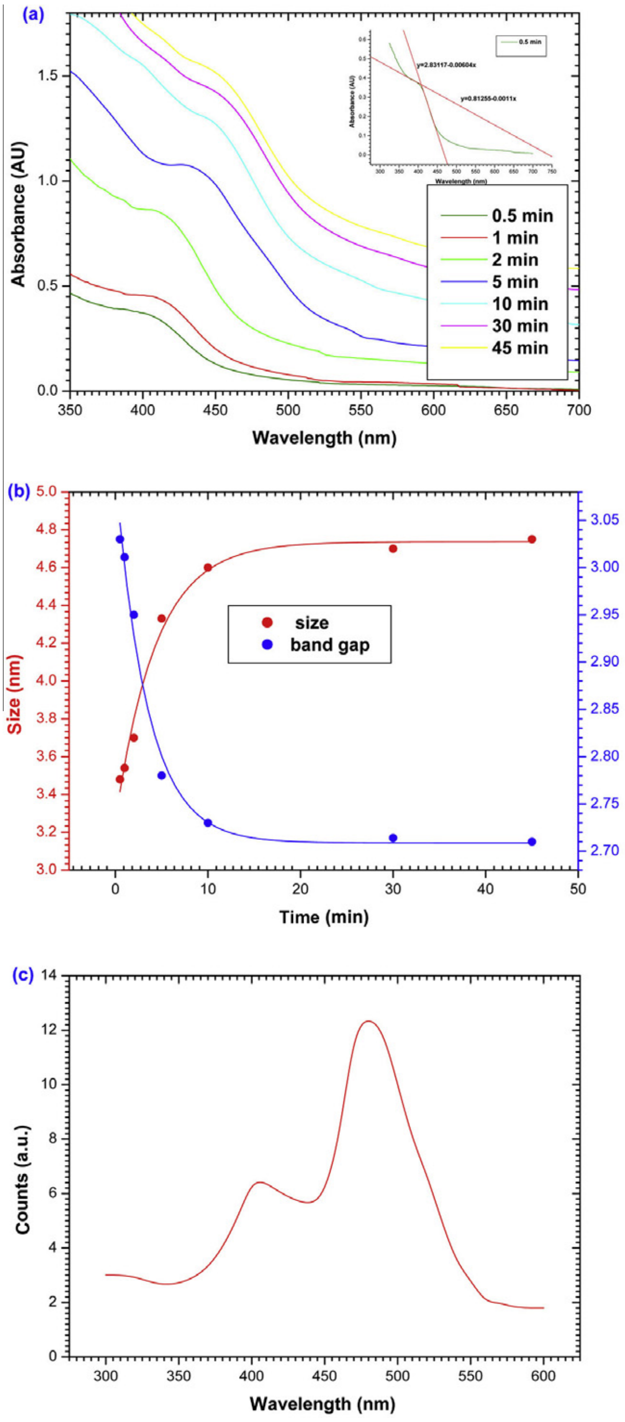

Fig. 7. (a) UV–visible spectra of samples at different interval times, (b) time of sonication on the optical size and band-gap of nano-particles, (c) photoluminescence spectrum of CdS nano-particle.

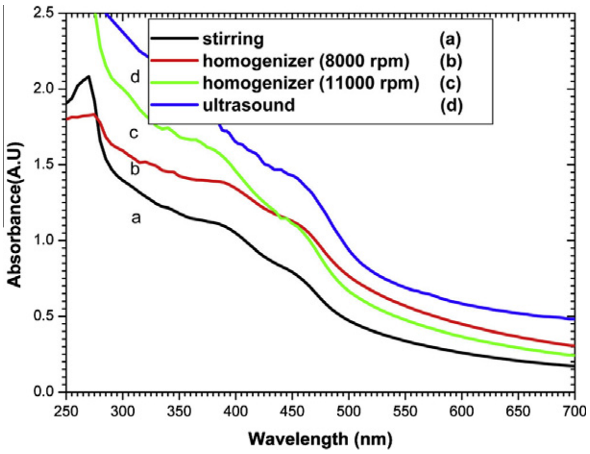

Fig. 8. UV–visible spectra of samples prepared in 30 min by different methods.

Table 4
Effect of kind of method on the surface and size of nano-particles in 30 min.

Method	Size crystal (XRD) (nm)	Optical size (nm)	Band-gap (eV)	Surface (m^2/g)
Ultrasound	2.10	4.66	2.72	152 ± 1
Homogenizer (11,000 rpm)	2.40	4.98	2.67	82.8 ± 0.6
Homogenizer (8000 rpm)	–	5.16	2.65	72 ± 2
Stirring	2.60	5.24	2.64	48.50 ± 0.03

In the case of intensity effect, there was an optimum intensity for higher surface area of nano-particles. The study of optical properties also confirmed that there is a specific relationship between particle size and energy band-gap.

Acknowledgments

The authors acknowledge the help given by Mrs. M. Hassanzadeh from Solid State Physics Research Center, Damghan University of Basic Sciences and Mrs. R. Pesyan from Central Research Laboratory of Ferdowsi University of Mashhad for analysis. This work has been supported by the "Iranian National Science Foundation: INSF" (No. 85103/31).

References

[1] D.V. Talapin, I. Mekis, S. Gotzinger, A. Kornowski, O. Benson, H. Weller, CdSe/CdS/ZnS and CdSe/ZnSe/ZnS core–shell–shell nanocrystals, J. Phys. Chem. B 108 (2004) 18826.
[2] P.V. Kamat, Quantum dot solar cells. Semiconductor nanocrystals as light harvesters, J. Phys. Chem. C 112 (2008) 18737.
[3] S.V. Pol, V.G. Pol, A. Gedanken, Encapsulating ZnS and ZnSe nanocrystals in the carbon shell: a RAPET approach, J. Phys. Chem. C 111 (2007) 13309.
[4] F. Caruso, Colloids and Colloid Assemblies, Wiley-VCH Verlag GmbH & Co. KGaA, Weinheim, 2004.
[5] J.L. Zhao, J.A. Bardecker, A.M. Munro, M.S. Liu, Y.H. Niu, I.K. Ding, J.D. Luo, B.Q. Chen, A.K.Y. Jen, D.S. Ginger, Efficient CdSe/CdS quantum dot light-emitting diodes using a thermally polymerized hole transport, Layer Nano Lett. 6 (2006) 463.
[6] A. Kubacka, B. Bachiller-Baeza, G. Colón, M. Fernández-García, W, N-codoped TiO_2–anatase: a sunlight-operated catalyst for efficient and selective aromatic hydrocarbons photo-oxidation, J. Phys. Chem. C 113 (2009) 8553.
[7] M. Bruchez, M. Moronne, P. Gin, S. Weiss, A.P. Alivisatos, Semiconductor nanocrystals as fluorescent biological labels, Science 281 (1998) 2013.
[8] L. Li, W. Wang, H. Liu, X. Liu, Q. Song, S. Ren, First principles calculations of electronic band structure and optical properties of Cr-doped ZnO, J. Phys. Chem. C 113 (2009) 8460.
[9] Y.J. Chan, S. Steckel, P.T. Snee, J.M. Caruge, J.M. Hodgkiss, D.G. Nocera, M.G. Bawendi, Blue semiconductor nanocrystal laser, Appl. Phys. Lett. 86 (2005) 073102.
[10] J. Schäfer, J.P. Mondia, R. Sharma, Z.H. Lu, A.S. Susha, A.L. Rogach, L. Wang, Quantum dot microdrop laser, Nano Lett. 8 (2008) 1709.
[11] X. Fan, M.L. Zhang, I. Shafiq, W.J. Zhang, C.S. Lee, S.T. Lee, Bicrystalline CdS nanoribbons, Cryst. Growth Des. 9 (2009) 1375.
[12] J.S. Jie, W.J. Zhang, Y. Jiang, X.M. Meng, Y.Q. Li, S.T. Lee, Photoconductive characteristics of single-crystal CdS nanoribbons, Nano Lett. 6 (2006) 1887.
[13] M. Sun, D. Li, W. Li, Y. Chen, Z. Chen, Y. He, X. Fu, New photocatalyst, Sb_2S_3, for degradation of methyl orange under visible-light irradiation, J. Phys. Chem. C 112 (2008) 18076.
[14] A. Datta, A. Priyam, S.N. Bhattacharyya, K.K. Mukherjea, A. Saha, Perature tunability of size in CdS nanoparticles and size dependent photocatalytic degradation of nitroaromatics, J. Colloid Interface Sci. 322 (2008) 128.
[15] Y. Liang, C. Zhen, D. Zou, D. Xu, Preparation of free-standing nanowire arrays on conductive substrates, J. Am. Chem. Soc. 126 (2004) 16338.
[16] J. Chen, X. Wang, Z. Zhang, In situ fabrication of mesoporous CdS nanoparticles in microemulsion by gamma ray irradiation, Mater. Lett. 62 (2008) 787.
[17] S.Q. Sun, T. Li, Synthesis and characterization of CdS nanoparticles and nanorods via solvo-hydrothermal route, Cryst. Growth Des. 7 (2007) 2367.
[18] G.Z. Shen, J.H. Cho, J.K. Yoo, G.C. Yi, C.J. Lee, Synthesis of single-crystal CdS microbelts using a modified thermal evaporation method and their photoluminescence, J. Phys. Chem. B 109 (2005) 9294.
[19] S. Kundu, H. Lee, H. Liang, Synthesis and application of DNA–CdS nanowires within a minute using microwave irradiation, Inorg. Chem. 48 (2009) 121.
[20] W. Xu, D.L. Akins, Reverse micellar synthesis of CdS nanoparticles and self-assembly into a superlattice, Mater. Lett. 58 (2004) 2623.
[21] E. Caponetti, D.C. Martino, M. Leone, L. Pedone, M.L. Saladino, V. Vetri, Microwave-assisted synthesis of anhydrous CdS nanoparticles in a water–oil microemulsion, J. Colloid Interface Sci. 304 (2006) 413.
[22] M. Ethayaraja, K. Dutta, D. Muthukumaran, R. Bandyopadhyaya, Nanoparticle formation in water-in-oil microemulsions: experiments, mechanism, and Monte Carlo simulation, Langmuir 23 (2007) 3418.
[23] R. Thiruvengadathan, Y. Levi-Kalisman, O. Regev, Synergetic effect of ultrasound and sodium dodecyl sulphate in the formation of CdS nanostructures in aqueous solution, Ultrason. Sonochem. 14 (2007) 398.
[24] M.P. Pileni, Reverse micelles as microreactors, J. Phys. Chem. 97 (1993) 6961.
[25] P. Zhang, L. Gao, Synthesis and characterization of CdS nanorods via hydrothermal microemulsion, Langmuir 19 (2003) 208.
[26] M.L. Curri, A. Agostiano, F. Mavelli, M. Della Monica, Reverse micellar systems: self organised assembly as effective route for the synthesis of colloidal semiconductor nanocrystals, Mater. Sci. Eng. C 22 (2002) 423.
[27] A. Tiehm, S. Krabnitzer, Y. Koltypin, A. Gedanken, Chloroethene dehalogenation with ultrasonically produced air-stable nano iron, Ultrason. Sonochem. 16 (2009) 617.
[28] T. Hyeon, M. Fang, K.S. Suslick, Nanostructured molybdenum carbide: sonochemical synthesis and catalytic properties, J. Am. Chem. Soc. 118 (1996) 5492.
[29] A.L. Morel, S.I. Nikitenko, K. Gionnet, A. Wattiaux, J. Lai-Kee-Him, C. Labrugere, B. Chevalier, G. Deleris, C. Petibois, A. Brisson, M. Simonoff, Sonochemical approach to the synthesis of Fe_3O_4@SiO_2 core–shell nanoparticles with tunable properties, ACS Nano 2 (2008) 847.
[30] R.V. Kumar, O. Palchik, Y. Koltypin, Y. Diamant, A. Gedanken, Sonochemical synthesis and characterization of Ag_2S/PVA and CuS/PVA nanocomposite, Ultrason. Sonochem. 9 (2002) 65.
[31] C. Wang, H. Zhang, J. Zhang, M. Li, H. Sun, B. Yang, Application of ultrasonic irradiation in aqueous synthesis of highly fluorescent CdTe/CdS core–shell nanocrystals, J. Phys. Chem. C 111 (2007) 2465.
[32] M.H. Entezari, N. Ghows, M. Chamsaz, Combination of ultrasound and discarded tire rubber: removal of Cr(III) from aqueous solution, J. Phys. Chem. A 109 (2005) 4638.
[33] M.H. Entezari, N. Ghows, M. Chamsaz, Ultrasound facilitates and improves removal of Cd(II) from aqueous solution by the discarded tire rubber, J. Hazard. Mater. B 131 (2006) 84.
[34] H. Wang, J.R. Zhang, J.J. Zhu, Sonochemical preparation of lead sulfide nanocrystals in an oil-in-water microemulsion, J. Cryst. Growth 246 (2002) 161.
[35] J.X. Huang, Y. Xie, B. Li, Y. Liu, J. Lu, Y.T. Qian, Ultrasound-induced formation of CdS nanostructures in oil-in-water microemulsions, J. Colloid Interface Sci. 236 (2001) 382.
[36] H. Wang, Y. Lu, J.J. Zhu, Preparation of cube-shaped CdS nanopartcles by sonochemical method, Int. J. Nanosci. 1 (2002) 437.
[37] G.C. De, A.M. Roy, S. Saha, S. Aditya, Semiconductor nanoparticles (CdS, ZnS and Zn^xCdS^{1-x}) in reverse micellar media, J. Indian Chem. Soc. 80 (2003) 551.
[38] K.-T. Yong, Y. Sahoo, M.T. Swihart, P.N. Prasad, Shape control of CdS nanocrystals in one-pot synthesis, J. Phys. Chem. C 111 (2007) 2447.
[39] M.W. Grinstaff, A.A. Cichowlas, S.B. Choe, K.S. Suslick, Effect of cavitation conditions on amorphous metal synthesis, Ultrasonics 30 (1992) 168.
[40] W.J. Erasmus, E. Steen, Some insights in the sonochemical preparation of cobalt nano-particles, Ultrason. Sonochem. 14 (2007) 732.
[41] S.G. Gaikwad, A.B. Pandit, Ultrasound emulsification: effect of ultrasonic and physicochemical properties on dispersed phase volume and droplet size, Ultrason. Sonochem. 15 (2008) 554.
[42] O. Kenji, Y. Akihiko, T. Shuji, M. Hiroshige, Y. Yoshihiro, Formation of colloidal gold nanoparticles in an ultrasonic field: control of rate of gold(III) reduction and size of formed gold particles, Langmuir 17 (2001) 7717.
[43] D. Jian, Q. Gao, Synthesis of CdS nanocrystals and Au/CdS nanocomposites through ultrasound activation liquid–liquid two-phase approach at room temperature, Chem. Eng. J. 121 (2006) 9.
[44] M. Moffitt, L. McMahon, V. Pessel, A. Eisenberg, Size control of nanoparticles in semiconductor–polymer composites. 2. Control via sizes of spherical ionic

microdomains in styrene-based diblock ionomers, Chem. Mater. 7 (1995) 1185.

[45] A. Rosencwaig, Photoacoustics and Photoacoustic Spectroscopy, Wiley, New York, 1980.

[46] S. Avivi (Levi), O. Palchik, V. Palchik, M.A. Slifkin, A.M. Weiss, A. Gedanken, Sonochemical synthesis of nanophase indium sulfide, Chem. Mater. 13 (2001) 2195.

[47] L. Brus, Electron–electron and electron–hole interactions in small semiconductor crystallites: the size dependence of the lowest excited electronic state, J. Chem. Phys. 80 (1984) 4403.

[48] M. Marandi, N. Taghavinia, A. Iraji zad, S.M. Mahdavi, Fine tuning of the size of CdS nanoparticles synthesized by a photochemical method, Nanotechnology 17 (2006) 1230.

[49] W. Xu, Y. Liao, D.L. Akins, Formation of CdS nanoparticles within modified MCM-41 and SBA-15, J. Phys. Chem. B 106 (2002) 11127.

[50] B.A. Harruff, C.E. Bunker, Spectral properties of AOT-protected CdS nanoparticles: quantum yield enhancement by photolysis, Langmuir 19 (2003) 893.